Coordination Chemistry Reviews 253 (2009) 410–422

Contents lists available at ScienceDirect

Coordination Chemistry Reviews

journal homepage: www.elsevier.com/locate/ccr

Review

Fluorescent conjugated polymer molecular wire chemosensors for transition metal ion recognition and signaling

Li-Juan Fan[a,b], Yan Zhang[a], Clifford B. Murphy[a], Sarah E. Angell[a], Matthew F.L. Parker[a], Brendan R. Flynn[a], Wayne E. Jones Jr.[a,*]

[a] Department of Chemistry, State University of New York at Binghamton, Vestal Pkwy East, Binghamton, NY 13902, United States
[b] School of Chemistry and Chemical Engineering, Soochow University, Suzhou 215123, People's Republic of China

Contents

ARTICLE INFO

Article history:
Received 20 April 2007
Accepted 13 March 2008
Available online 21 March 2008

Keywords:
Fluorescent chemosensor
Conjugated polymer
Molecular wire
Electron transfer
Energy transfer
Fluorescent enhancement and quenching

ABSTRACT

Conjugated polymer molecular wires have advantages over small molecules for sensing applications due to enhancements associated with electronic communication along the polymer backbone. The majority of examples from the literature focus on fluorescence "turn-off" as the mechanism of sensor response. The energy transfer mechanism involved in these polymers focuses on energy transfer quenching and can be related to either a Dexter or Förster based mechanism. More recently, a series of chemosensors have been designed and synthesized which exhibit fluorescence "turn-on" behavior upon binding specific cations. The general assembly of both the turn-on and turn-off chemosensor structures involves assembling different organic receptor ligands onto the conjugated polymer backbones. Careful spectroscopic analysis of the energy and electron transfer mechanisms in these systems creates a myriad of opportunities for the design of new sensor materials.

* Corresponding author. Tel.: +1 607 777 2421; fax: +1 607 777 4478.
E-mail address: wjones@binghamton.edu (W.E. Jones Jr.).

0010-8545/$ – see front matter © 2008 Elsevier B.V. All rights reserved.
doi:10.1016/j.ccr.2008.03.008

1. Introduction

1.1. Fluorescent chemosensors

Great effort has recently been devoted to the design and construction of molecular sensory systems for a broad range of environmental and biological analyses [1–12]. A sensor is defined by the Oxford English Dictionary as "a device that detects or measures a physical property and records, indicates or otherwise responds to it". A sensor achieves this goal by responding to an external stimulus and converting it into a signal which can be measured or recorded. A chemical sensor is a device that qualitatively or quantitatively detects the presence of specific chemical substances, a class of chemicals or a specific chemical reaction.

Generally, a sensor device contains three elements: a receptor, a signal transducer and a read-out (Fig. 1). The receptor should have the ability to discriminate and bind a specific target substance known as the analyte. Successful, selective receptor–analyte complex formation depends on the size, shape and binding energy of the receptor and analyte molecules. Signal transduction is the process through which an interaction of receptor with analyte yields a measurable form of energy change and is converted to a signal change that can be read and quantified. The read-out domain is the part responsible for reporting the binding event. Some parameters that define a sensor's performance are selectivity, sensitivity, stability, reproducibility and cost.

A chemosensor is a chemical sensor based on one molecule if we view one individual molecule as one engineered molecular device. It has been defined as a molecule of abiotic origin that signals the presence of a target chemical substance [7]. The three elements of a sensor device are not necessarily independent and physically separated into the three components. Sometimes, one part of the molecule can act as a combination of two or more elements.

Fluorescence is the emission of photons following relaxation from an excited electronic state to the ground state [13]. Chemosensors based on fluorescence signal changes are commonly referred to as fluorescent chemosensors [7]. Fluorescent chemosensors are gaining increased attention due to their high sensitivity and ease of measurement [5–12]. Fluorescent chemosensors are usually made up of three components: a receptor, a fluorophore and a spacer to link them together. These three parts do not exactly correspond to the three components shown in Fig. 1. In most cases, the spacer is not responsible for signal transduction. The read-out of a fluorescent chemosensor usually is measured as a change in fluorescence intensity, intensity decay lifetime, or a shift of the emission wavelength. An important feature of the fluorescent chemosensors is that signal transduction of the analytes binding event into the readout can happen in a very short time and without any other assistance. This makes real-time and real-space detection of the analyte possible as well as imaging associated with analyte distribution. In this review, we will restrict our discussion to those sensors based on a change in fluorescence emission intensity.

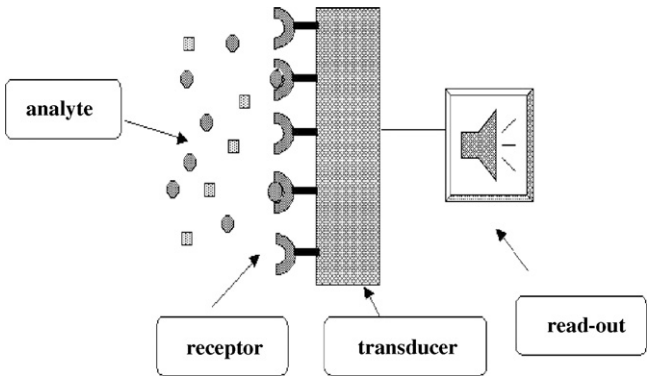

Fig. 1. Schematic illustration of a sensor device (especially a chemical sensor device).

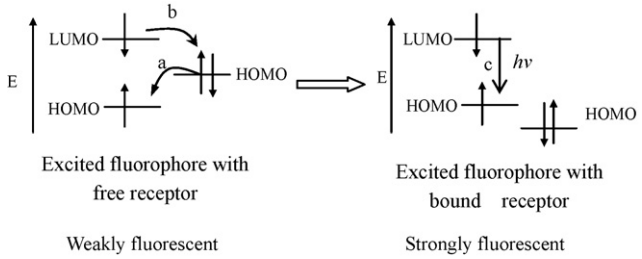

Fig. 2. Orbital energy diagrams for fluorescence "turn-on" PET sensors before and after binding cation and (a) forward electron transfer; (b) backward electron transfer; (c) fluorescence emission processes.

1.2. Mechanism of analyte detection

There are several mechanisms of fluorescence sensing. Photoinduced electron transfer (PET) and electronic energy transfer (EET) are mechanisms that have been extensively studied and widely used in the design of the chemosensors. Both mechanisms result in changes in fluorescence intensity. This review will be focused on the detection of cations by either mechanism. These sensing mechanisms are applicable to a broad array of analytes as has been reviewed previously [8–10].

1.2.1. Photoinduced electron transfer

Photoinduced electron transfer sensors can be classified into two categories: fluorescence "turn-on" or fluorescence "turn-off" upon binding cations. For fluorescence "turn-on" sensors, the receptors usually contain a relatively high-energy non-bonding electron pair. In the absence of analytes, this electron pair quenches the emission by rapid intramolecular electron transfer from the receptor to the excited fluorophore, as shown in Fig. 2. When this electron pair coordinates to Lewis acid cations in solution, the HOMO of the receptor is lowered. This decreases the driving force for the PET process effectively stopping the quenching event and turning on the fluorescence of the chromophore.

In some cases, the receptor takes part only indirectly in the photophysical process. If the energy level of the cation LUMO is between the energy levels of the fluorophore HOMO and LUMO, the binding of the cations by the receptor provides a non-radiative path to dissipate the excitation energy, resulting in a quenching of the fluorescence of the chemosensor (Fig. 3).

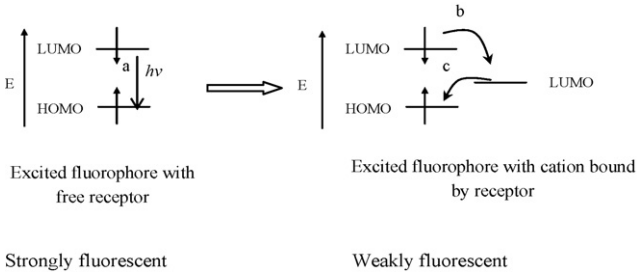

Fig. 3. Orbital energy diagrams for fluorescent "turn-off" PET sensors before and after binding cation and (a) fluorescence emission; (b) forward electron transfer; (c) backward electron transfer processes.

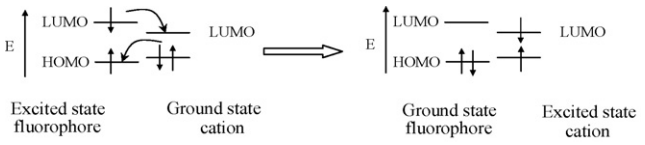

Fig. 4. Orbital energy diagrams for double exchange transfer between the excited fluorophore to the cation bound by receptor followed by cation return to the ground state by non-radiative decay.

The difference between these two mechanisms is that the PET process takes place either before or after the cation binding. For the "turn-on" sensor, the PET process is participated in by the HOMO, LUMO of the fluorophore and the HOMO of the receptor before cation binding. For the "turn-off" sensor, the PET process involves the HOMO, LUMO of the fluorophore and the LUMO of the cation after complex formation.

1.2.2. Electronic energy transfer

Electronic Energy transfer is another mechanism for the fluorescence quenching upon binding cations. There are two kinds of EET mechanisms: the double electron exchange (Dexter) energy transfer or the dipole–dipole coupling (Förster) energy transfer [12,13]. In the organic fluorophore–cation system, usually the Dexter energy transfer dominates as shown is Fig. 4. In this case, the fluorophore goes back to its ground state by non-radiative decay. The Dexter energy transfer requires close contact between the fluorophore and the cations and also direct orbital overlap. This type of fluorescence quenching not only requires the appropriate relative energy levels between fluorophore and cation, but also requires some specific characteristics of the spacer, such as flexibility and a shorter distance between the donor and acceptor.

The Förster energy transfer mechanism involves the long range coupling of dipoles, allowing for an exchange of excitation energy through space, i.e. without a path of direct orbital overlap. These two mechanisms of energy transfer are differentiated primarily in their dependence on the distance between the donor and acceptor states, shown qualitatively in Fig. 5. The Förster mechanism is more likely to occur at extremely short and extremely long distances. For most chemosensory systems where conjugation is involved, the Dexter mechanism of direct orbital overlap is expected to be dominant [13–15].

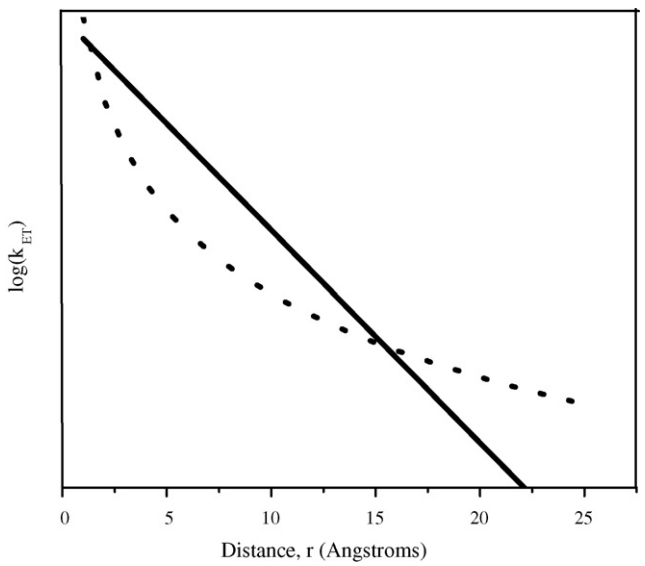

Fig. 5. Plot of $\log(k_{ET})$ vs. distance, r, for both Dexter (solid line) and Föster (dotted line) energy transfer mechanism, absent any criteria other than distance. k_{ET} donates the rate of energy transfer.

1.3. Conjugated polymers as molecular wires

The concept of a molecular wire has been discussed for over 30 years since it was first discovered that conjugated polymers could be prepared as electrical conductors [16,17]. In conjugated polymers, each carbon atom along the backbone has sp or sp^2 hybridization. The remaining p orbitals, with one unpaired π electron each is placed side by side to form π bonds. Since the orbitals of successive carbon atoms along the backbone overlap, the π electrons are delocalized along the polymer backbone. This electronic delocalisation provides a pathway for electron or hole mobility along the backbone of the polymer chain.

Recently, there has been renewed interest in the developing of conjugated polymer molecular wires for their applications in organic light emitting diodes [18–22], photovoltaics [23–26], actuators [27], batteries [28–30], and field-effect transistors [31]. This wide range of applications is the result of the unique metallic and semiconducting properties inherent to many of these conjugated polymer systems. An interesting recent extension of these materials has been their subsequent application to fluorescent sensors [5,6,32–35]. Numerous studies have been made on the properties and applications of conjugated polymers such as poly(acetylene)poly(*p*-phenylenevinylene) (PPV) [36–38], poly(*p*-phenyleneethylene) (PPE) [5,6,32] and polythiophene (PT) [39,40]. Several groups have investigated the structure–property relationships of poly[*p*-(phenyleneethynylene)-*alt*-(thienyleneethynylene)] (PPETE) [41,42]. The PPETE structure has been found to be highly luminescent and also have very good possibility. They deviate slightly from the PPE rigid-rod structure due to the inclusion of the five-member thiophene ring, but still have a relatively high degree of π electron delocalisation [41,42].

1.4. Conjugated polymer sensors vs. small molecule sensors

Small molecules as fluorescence sensors have been extensively studied in the past several decades [8–12]. The most commonly used fluorophores are aromatic compounds, especially anthracene [43]. Recently, conjugated polymer chemosensors have been used with great success for detection of a range of analytes from biomolecules to explosives [32,44–48]. Conjugated polymers, or molecular wires, have several advantages over small molecules for sensing applications due to enhancements associated with electronic communication between receptors along the polymer backbone, processibility and ease of structural modification.

Conjugated polymer sensors have been classified based on various transduction principles such as conductometry, potentiometry, chemical field-effect transistor (CHEMFET) and fluorescence [33,49,50]. Here we will focus our discussion on conjugated polymers as fluorescence chemosensors. In some cases, conjugated polymer fluorescence shows a direct response to an external analyte and the conjugated polymers can be used directly as fluorescent sensors. The combination of the sensitivity of fluorescence and unique properties of conjugated polymers provides new opportunities for sensory system development. One type of conjugated polymer fluorescent sensor is based on the conformational change of conjugated backbone driven by interaction with the analyte. For instance, the fluorescence of poly[3-oligo(oxyethylene)-4-methythiophene] changes in the presence of alkali metals and the intensity of fluorescence is a function of the concentration of alkali metal cations [51]. Another type of conjugated polymer sensor involves the introduction of molecular recognition units (recep-

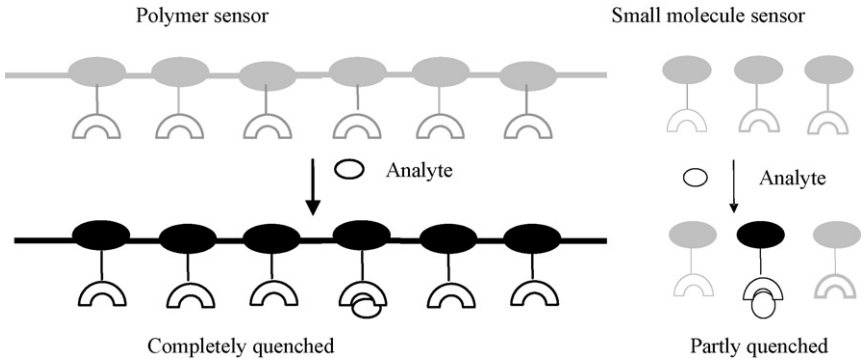

Fig. 6. This schematic representation demonstrates sensory signal amplification using the molecular wire approach.

tors) on the polymer. The receptors can be either in the polymer backbone or as pendants. An elegant example of the former is the polymer synthesized by Wang and Wasielewski [52]. A bipyridyl group with a dihedral angle of 20° was introduced into the polymer backbone. Chelation to transition metal ions increases the planarity of the bipyridyl site and the conjugation length. Hence the conformational change can be monitored by UV–vis and fluorescence spectroscopy.

Polymers offer a great deal of flexibility in their synthesis and utility. Assembling the receptor pendants through the conjugated polymer backbone is another excellent approach to amplifying the fluorescent signals [32,47,48]. As illustrated in Fig. 6, the receptors are connected by the conjugated polymer-'molecular wire'. Analyte binding produces energy trap sites for the fluorescent excitons. Due to the facile energy migration, in which excitons diffuse along the conjugated polymer backbone, the emission intensity of conjugated polymers decreases dramatically [32,53]. By utilizing the collective properties of the molecular wire configuration containing multiple receptors, one can achieve enhanced sensitivity of polymer fluorescent sensors relative to small molecule sensors. This concept was first advanced and demonstrated by Swager's group [47,48]. They assembled the cyclophane-based receptors onto a *para*-poly(phenyleneethynylene) backbone and this polymer showed a 65-fold fluorescence enhancement in sensitivity to paraquat, compared to a model fluorescent chemosensor containing only one receptor.

This signal amplification creates a chemosensor that is significantly more sensitive to analytes than its single molecule counterparts. The phenomenon of energy transfer enhancement essentially allows one binding event to quench the fluorescence of multiple fluorescence sensor sites on the chain. In this review we are going to focus on the research carried out in our lab using conjugated polymers as the backbone combined with different receptors as transition metal ion chemosensors. All the photophysical measurements of the polymer and including the titration with metal cations were carried out in tetrahydrofuran (THF). The THF solvent was an ideal carrier based on the high solubility of the polymer and its miscibility with H_2O, which was the target medium for cation detection in the environment.

2. Conjugated polymers as fluorescence "turn-off" chemosensors

The toxicity of certain metal ions has been a constant cause of environmental concern. Thirteen transition metal ions are listed as "priority pollutants" by the Environmental Protection Agency (EPA) [54]. There is an increasing need for development of field-based sensors and remediation devices, demanding new chemosensory materials and novel low cost synthetic designs for detecting these cations. Lewis bases such as pyridyl ligands are known to coordinate a large number of transition metal ions [55]. There are only a limited number of reports involving incorporating pyridyl ligands into conjugated polymers as chemosensors [52,56]. We have successfully designed and synthesized a series of new chemosensory polymers, poly[*p*-(phenyleneethynylene)-*alt*-(thienyleneethynylene)] with different oligopyridine pendant groups as receptors for transition metals (Fig. 7) [57]. These systems take advantage of the strong conjugation and luminescence properties of the polyarylene ethynylene backbone together with the multi-dentate Lewis base coordinating ability of oligo-pyridines to yield a highly effective transition metal chemosensor. Among all the polymers, tolylterpyridine-poly[*p*-(phenyleneethynylene)-*alt*-(thienyleneethynylene) (ttp-PPETE) showed the highest sensitivity of fluorescence quenching towards cations. In this review, we will restrict our discussion to the ttp-PPETE system since it was demonstrated to have the best performance as a chemosensor.

To quantify the emission quenching relative to the concentration of the cations, a Stern–Volmer analysis was carried out in the ttp-PPETE system. Based on Stern–Volmer analysis, we have also advanced a new mathematical model to explain the enhanced quenching of our polymer system by cations [58]. This model helped us to achieve a better understanding of energy-transfer processes in conjugated polymer sensors and also could be helpful in the design of new, more sensitive, chemosensory materials. Exploration was also carried out on the different percent loading of the receptor tolylterpyridine (ttp) onto the PPETE polymer backbone [59,60]. This was based on the concept that increasing the distance between the receptors on the polymer backbone may exploit energy transfer to enhance cation quenching sensitivity.

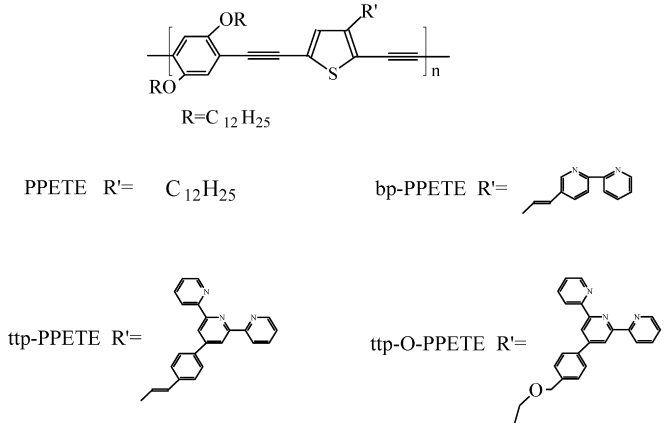

Fig. 7. Molecular structure of the PPETE polymers is shown here with oligo-pyridine pedants.

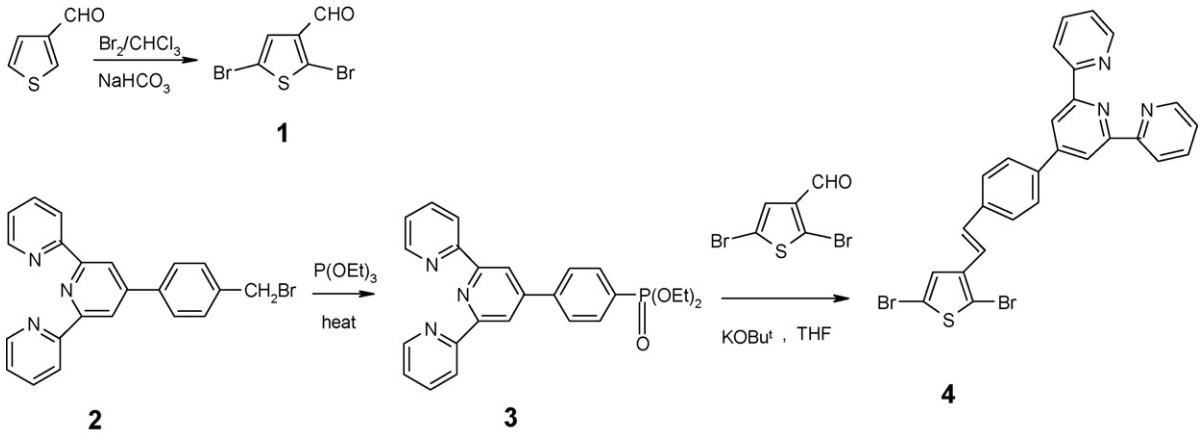

Scheme 1. Synthesis of the terpyridine-loaded monomer (see Ref. [57]).

2.1. Preparation

To synthesize the PPETE polymers using a Pd-catalyzed cross coupling reaction [61–63], the corresponding monomers, aryl halide and aryl acetylene are needed. Compound 1,4-diethynyl-2,5-didodecyloxybenzene (**5**) (see Scheme 2) was used as one building block and was synthesized according to the literature [64]. The long alkoxy chains of this compound provide the solubility of the polymers in most organic solvents. The synthetic sequence of the other building block, 2,5-dibromo-thiophene unit, is outlined in Scheme 1. Transition metal receptor terpyridyl groups were introduced to the thiophene rings by the Horner–Wittig–Emmons reaction [65]. To this end, 4′-(*p*-bromomethylphenyl)-2,2′:6′2″-terpyridine was easily synthesized from 4′-*p*-tolyl-2,2′:6′2″-terpyridine by the literature procedure [66]. The compound 2,5-dibromo-thiophene-3-carbaldehyde (**1**) was readily synthesized from the reaction of 3-thiophenecarboxaldehyde with Br_2 in the presence of $NaHCO_3$. Terpyridine phosphite (**3**) was prepared by reacting 4′-(p-bromomethylphenyl)-2,2′:6′2″-terpyridine (**2**) with triethyl phosphite, and subsequently treated *in situ* with 2,5-dibromo-3-thiophenecarboxaldehyde (**1**). This produces the monomer 4-{4-[2-(2,5-dibromo-thiophen3-yl)-vinyl]-phenyl}-[2,2′:6′,2″]terpyridine (**4**) with 80% yield.

Polymerization was accomplished by employing palladium-catalyzed cross-coupling [61–63] of 1,4-diethynyl-2,5-didodecyloxybenzene (**5**), and 4′-{4-[2-(2,5-dibromo-thiophen3-yl)-vinyl]-phenyl}-[2,2′:6′,2″]terpyridine (**4**), as shown in Scheme 2. The model PPETE was synthesized under the same conditions with monomer 1,4-diethynyl-2,5-didodecyloxybenzene (**5**) and monomer 2,5,-dibromo-3-dodecyl-thiophene which is commercially available or 2,5-diiodo-3-dodecyl-thiophene, which was synthesized in our lab.

2.2. Fluorescence quenching in the ttp-PPETE system

Typical absorbance spectra for the PPETE and ttp-PPETE systems in THF solution are shown in Fig. 8. The PPETE model backbone has a strong absorbance maximum around 440 nm and a weaker absorbance at 325 nm. Both of these transitions have previously been assigned to π–π^* transitions in the conjugated polymer backbone [41,42,57,58]. The ttp-PPETE polymer exhibits an additional strong absorbance at 340 nm consistent with the absorption that is observed for the π–π^* transition in the tolyterpyridyl pendant. Upon addition of the terpyridyl group, a distinct red shift is observed for the lowest energy relative to the model PPETE backbone. This shift is consistent with an increase in the overall conjugation along the backbone.

Due to the varying chelating ability of terpyridine with different transition metals, this polymer shows some selectivity towards different transition metals. The polymer ttp-PPETE shows some sensitivity to several transition metal ions such as Cr^{6+}, Cd^{2+}, Ni^{2+}, and Mn^{2+} (Fig. 9). It should be noted that in the case of Cr^{6+}, the metal ion is sampled from the Aldrich AA Standard solution for Cr^{6+},

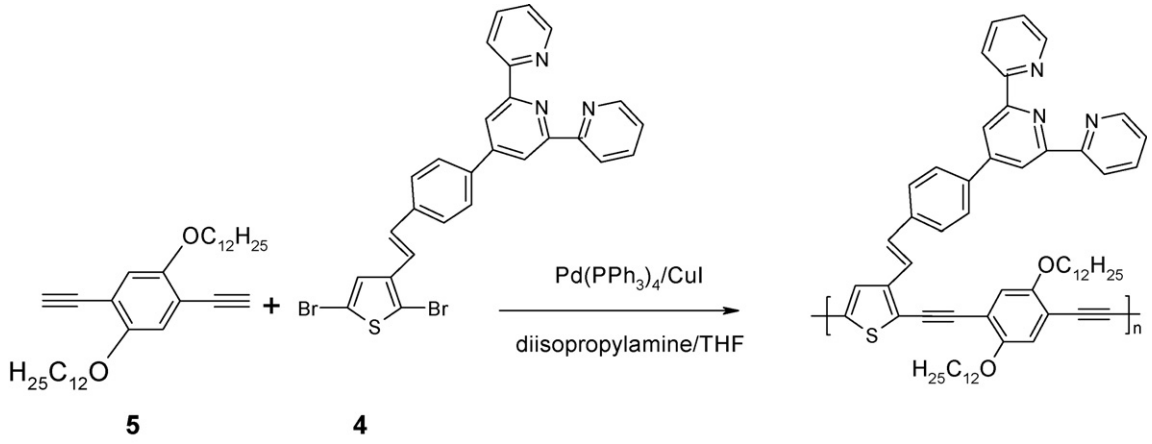

Scheme 2. Synthesis of ttp-PPETE chemosensor polymer (see Refs. [57,58]).

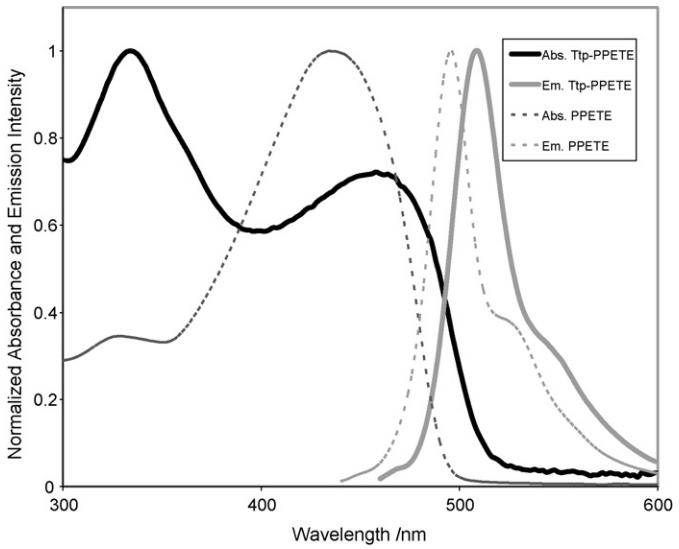

Fig. 8. Normalized absorbance and emission profiles for PPETE and ttp-PPETE polymers are shown in THF at room temperature (adapted from Ref. [57]).

which is a solution of dichromate ion in acidified solution [57]. In these experiments, both receptor of ttp-PPETE polymer and transition metal quencher concentrations were held fixed at 3.08 μM and 1.54 μM, respectively. The polymer was quenched to 29.0% of its initial intensity in the presence of Ni^{2+} under these conditions, while 79.6% of the intensity remained when Cd^{2+} was used as the quencher. No quenching was observed in the presence of common cations such as Na^{+} or Ca^{2+}. The polymer was also not responsive to competing contaminants such as Pb^{2+} or Hg^{2+}.

A representative spectral series of quenching data for ttp-PPETE as a function of Ni^{2+} concentration in THF solution is shown in Fig. 10. In these experiments, the terpyridyl receptor concentration was held fixed at 5.0 μM. We have observed appreciable emission quenching for Ni^{2+} concentrations as low as 4 nM (not shown in this figure). The emission intensity decreases (intensity change at λ_{max}) to about 60% of the initial intensity at Ni^{2+} concentrations as low

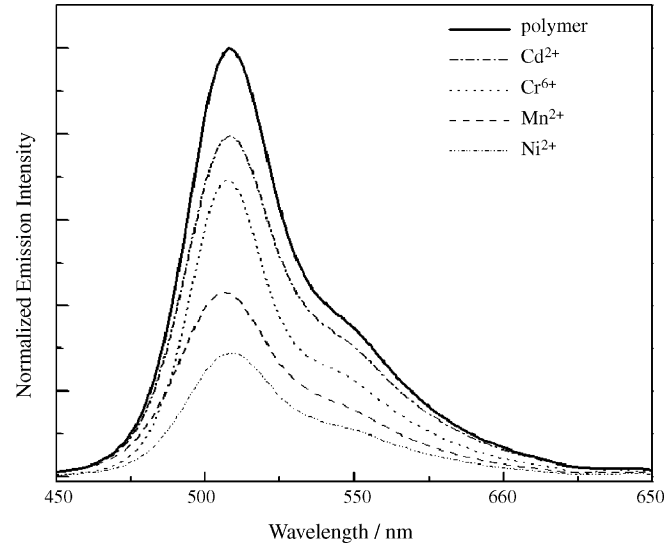

Fig. 9. Emission quenching of ttp-PPETE polymer is shown in the presence of different transition metal ions. Polymer concentrations are held fixed at 3.08 μM corresponding to receptor unit. Concentration of transition metal ions is 1.54 μM and normalized relative to the polymer in the absence of metal quenchers (adapted from Ref. [57]).

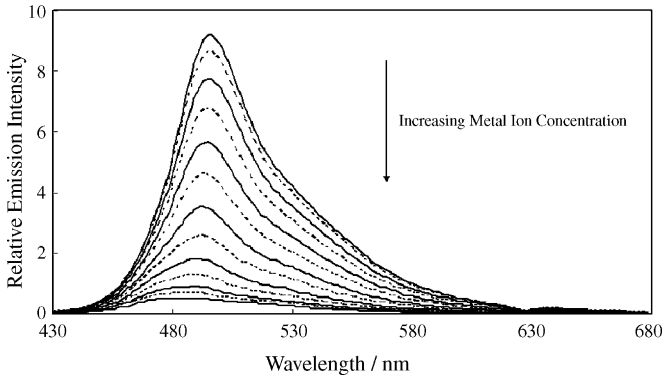

Fig. 10. Emission spectra recorded in THF at room temperature for Ni^{2+} complexes with ttp-PPETE. Emission intensity decays are for increments of 0.25 μM additions of Ni^{2+} analyte. The polymer concentration is 5.0 μM corresponding to receptor unit (adapted from Ref. [57]).

as 1.0 μM. In addition, there is a small blue shift in emission energy with suggests a shortening of the exciton migration distance with increasing quencher loading.

2.3. Stern–Volmer and energy transfer migration analysis of the ttp-PPETE system

2.3.1. Stern–Volmer analysis

The nature of the quenching in ttp-PPETE was characterized by Stern–Volmer analysis [13,14]. A variety of molecular interactions can result in quenching. Quenching originating from collisional interaction between the fluorophore and quencher is called collisional or dynamic quenching. Dynamic quenching can be described by the Stern–Volmer equation

$$\frac{I_0}{I} = \frac{\tau_0}{\tau} = 1 + k_q \tau_0 [Q] \quad (1)$$

where I_0 is the initial emission intensity in the absence of quenchers, I the emission intensity, k_q the rate of dynamic (collisional) quenching, τ_0 the lifetime of the fluorophore in the absence of the quenchers, τ the lifetime in the presence of quenchers, and [Q] is the quencher concentration in solution.

Another type of quenching occurs as a result of the formation of a non-fluorescent complex between the fluorophore and quencher. For this type of quenching, the decrease of fluorescence intensity has the same form as the Stern–Volmer equation above. However, in Eq. (2) the K_{SV} is now the association constant K_S. Since the lifetime of the fluorophore is unperturbed by the static quenching, $\tau_0/\tau = 1$, lifetime measurements are a definitive method to distinguish between static and dynamic quenching [13,14].

$$\frac{I_0}{I} = 1 + K_{SV}[Q] \quad (2)$$

Stern–Volmer analysis of the quenching experiment (I_0/I vs. [Ni^{2+}]) is shown in Fig. 11. It is interesting to note the non-linear nature of the Stern–Volmer plot in this figure. Dynamic quenching processes would be expected to give a straight line with a *Y*-intercept of 1. Lifetime study shows that in the presence of metal ions, the ttp-PPETE lifetime remained bi-exponential with little shift in each lifetime component, suggesting that in this case, the mechanism of the quenching process involves complexation (static quenching) rather than collisional deactivation (dynamic quenching). Similar non-linear behavior that shows an upward deviation from the typically linear Stern–Volmer plot was also observed with Co^{2+}, Fe^{2+}, Cr^{6+}, Zn^{2+}, Cu^{2+}, Mn^{2+} and Fe^{3+}. However, Ni^{2+} showed the strongest response with the ttp-PPETE.

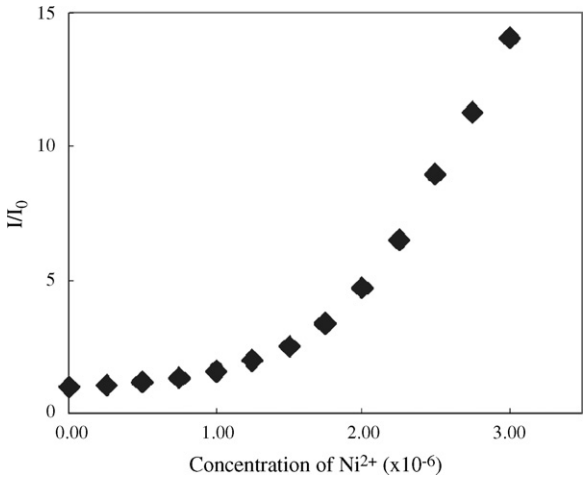

Fig. 11. A Stern–Volmer plot is shown demonstrating the fluorescence quenching of ttp-PPETE by Ni^{2+} in THF at room temperature. The polymer concentration is 5.0 μM corresponding to receptor unit (adapted from Ref. [57]).

2.3.2. Energy-transfer migration enhanced Stern–Volmer analysis

Non-linear behavior for polymer based fluorescence quenching has been observed previously [53,67,68]. A significant enhancement in quenching behavior has long been noted for polymers, where energy transfer migration along the polymer backbone is possible. The energy transfer process is illustrated using the state diagram shown in Fig. 12. The initial excitation leads to formation of an exciton which can rapidly migrate between *iso*-energetic sites along the conjugated polymer backbone to a low energy acceptor site. The result is an efficient fluorescence quenching mechanism even at very low quencher concentrations, since the binding of one receptor site leads to efficient quenching of several emitting units along the polymer backbone.

Increased sensitivity in the ttp-PPETE system was expected to arise from energy transfer migration along the backbone. Energy transfer migration enhancements to emission quenching have long been known for dynamic quenching systems. However, as described previously, ttp-PPETE showed static quenching with cations. Based on our experiments, observations and previous theoretical studies by Webber and co-workers [69], we advanced a new model to describe fluorescence quenching in our polymer systems, starting with adding an energy transfer factor into the conventional Stern–Volmer equation [58].

$$\frac{I}{I_0} = 1 + K_{SV}[Q] + k_{ET}\tau_f[Q] \tag{3}$$

In this equation K_{SV} is the static Stern–Volmer constant, [Q] the concentration of quencher, k_{ET} the rate of energy transfer, and τ_f is the lifetime of the non-quenched fluorophore. In this case, the K_{SV} term accounts for fluorescence loss only for the static, metal-bound receptor sites, and the k_{ET} term accounts for energy transfer from excitons that are not immediately adjacent to the metal-bound receptor site. By considering the distance dependence and mechanism of the energy transfer quenching, we then derived a set of equations (Eqs. (4) and (5)) based on either the Dexter or the Förster energy transfer mechanisms.

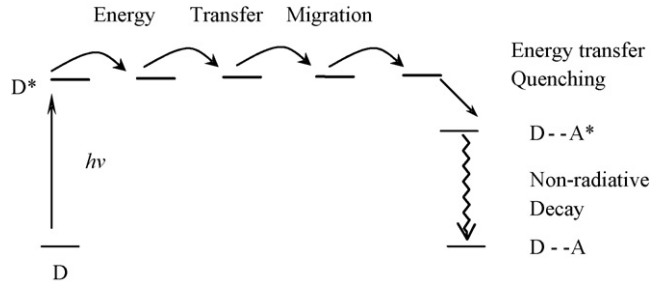

Fig. 12. Illustration of energy transfer migration quenching through a conjugated polymer.

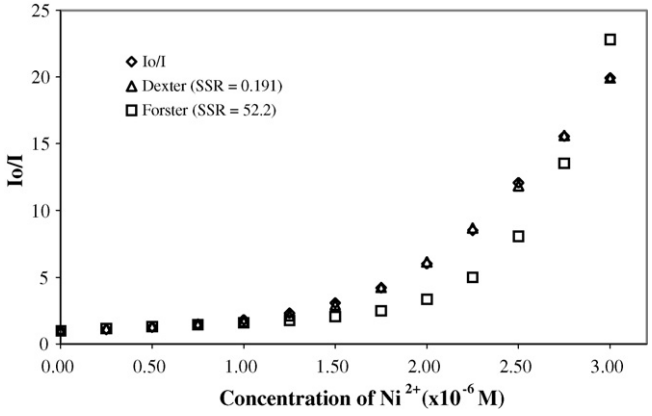

Fig. 13. Analysis of the Stern–Volmer quenching of 5.0×10^{-6} M ttp-PPETE in THF with Ni^{2+} by Dexter (Eq. (4)) or Förster (Eq. (5)) energy transfer mechanisms, respectively (adapted from Ref. [58]).

$$\frac{I_0}{I} = 1 + K_{SV}[Q] + \tau_f[Q]K'^2 \exp\left(\frac{-2r}{L}\right) \tag{4}$$

$$\frac{I_0}{I} = 1 + K_{SV}[Q] + \left(\frac{R_0}{r}\right)^6[Q] \tag{5}$$

Eq. (4) describes the energy transfer enhancement for the Dexter mechanism, where K' is a combination of constants with units of energy, r the average residue-repeat distance between quenchers, and L is a constant called the average effective Bohr radius. Eq. (5) is the analogous energy transfer enhancement for the Förster mechanism, where R_0 is the Förster critical distance, defined as the distance where energy-transfer is 50% likely to occur. It should be noted that the constants K' and R_0 both contain the overlap integral between the donor-fluorophore emission and acceptor absorbance profiles. These equations were successfully used to model the experimentally observed Stern–Volmer data (Fig. 13 and Table 1) [58].

On the basis of this model, it was demonstrated that different energy-transfer mechanisms exist as a function of the chemical identity of the analytes. For instance, the fluorescence quenching of ttp-PPETE in the presence of Ni^{2+} was best modeled through a Dexter type mechanism while the fluorescence quenching of ttp-PPETE in the presence of Co^{2+}, however, was best modeled through a Förster mechanism. Through careful tuning of the receptor interactions with both the polymer backbone and the analyte, it may

Table 1
Stern–Volmer constants and energy-transfer parameters for fits of quenching data for 5.00×10^{-6} M ttp-PPETE in THF

Analyte	K_{SV}[a] ($\times 10^5$)	R_0[b,c]	K'[c] ($\times 10^3$)	L[b]
Ni^{2+}	5.91	22.9 (52.2)	12.0 (0.191)	1.57
Co^{2+}	9.06	15.1 (11.2)	65.8 (17.8)	0.41
Cu^{2+}	2.01	22.1 (17.6)	11.7 (30.0)	0.49
Fe^{2+}	1.49	14.2 (999)	5.81 (1.35)	3.59

[a] in M^{-1}.
[b] in monomer unit lengths, *l*.
[c] SSR values in parentheses.

therefore be possible to create a more selective system for future chemosensory polymers.

2.4. Receptor loading dependence

A polymer series consisting of 100%, 50%, 33% and 25% terpyridine loaded PPETE backbones was synthesized [59,60]. Generally speaking, the polymer series was found to exhibit enhanced sensitivity to nickel ions with an increase in receptor spacing. This was demonstrated by an increase in the slope of the Stern–Volmer analysis carried out at low concentrations of the cation analyte. While this result suggests that uniform decrease in the loading would be advantageous, it was also observed that residual fluorescence also increased with receptor spacing. This challenge would need to be overcome at lower loading levels in order to construct an efficient sensor.

3. Conjugated polymers as fluorescence "turn-on" chemosensors

Most literature reports use fluorescence quenching as the readout mechanism for the sensing response. Relatively few involve a fluorescence "turn-on" response towards cations [70–74]. The greatest advantage of fluorescence "turn-on" sensors related to "turn-off" sensors is the ease of measuring low concentration contrast relative to a "dark" background. This reduces the likelihood of false positive signals as that could result from contaminants that would quench the fluorescence. Small molecules as fluorescence turn-on sensors based on photoinduced electron transfer have been well studied [74–78]. Based on our previous work using poly[*p*-(phenyleneethylene)-*alt*-(thienyleneethynylene)] as a conjugated polymer backbone and functionalizing it with different receptors [57,58], we advanced a strategy to synthesize a series of fluorescence "turn-on" polymer sensors with the PPETE polymer backbone as the fluorophore and different amino groups as the receptors [79]. With this synthetic strategy, we seek to develop an addressable family of conjugated polymer PET sensors that respond to different analytes by the "turn-on" mechanism (see Section 1.2.1). The first two polymers, dea-PPETE and tmeda-PPETE, were synthesized according to this strategy, using *N*,*N*-diethylamino and *N*,*N*,*N*′-trimethylethylenediamino groups as receptors, respectively (Fig. 14).

The polymer tmeda-PPETE showed varying fluorescence "turn-on" behavior in the presence of most cations. However, dea-PPETE showed only some limited fluorescence "turn-on" effect upon coordinating to cations. The different behavior of these two polymers could be attributed to two effects: the first is the different PET driving force due to the different energy level of the electron of the amino groups before cation binding [77,80–83]. The second is

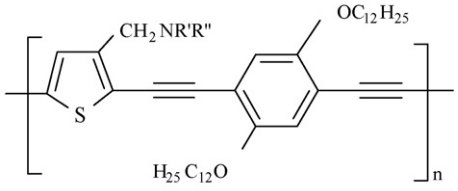

dea-PPETE NR'R"=N(CH_2CH_3)$_2$

tmeda-PPETE NR'R"=N(CH_3)CH_2CH_2N(CH_3)$_2$

Fig. 14. Structures of PPETE polymers with amino pendants.

that the higher equilibrium constant for binding could also account for the enhanced fluorescence "turn-on" behavior for tmeda-PPETE [84]. The following discussion will focus on the tmeda-PPETE system.

The factors which affect the sensitivity of a fluorescence "turn-on" system may be different from those in a "turn-off" system. Understanding the nature of these factors will be critical to the design of new conjugated polymer based "turn-on" sensors. One important issue is the efficiency of the PET process in this conjugated polymer backbone-receptor system. In a PET system, the HOMO-LUMO energy levels of the polymer fluorophore are very critical and HOMO-LUMO levels may change with the chain length. Another fundamental question about the PET based "turn-on" conjugated polymer system is how the intrachain energy transfer or energy migration along the polymer chain affects the total quenching of the polymer fluorescence by the receptor. To address this question, a series of polymers were prepared with variable loading of the amino receptor unit. The PET process between the PPETE polymer backbone and the receptor and the energy migration on the PPETE backbone with the amino receptor as a function of loading were also investigated [85].

In most cases, a "turn-on" system with very high sensitivity is not easy to be achieved due to the high "background" fluorescence, as described by Swager et al. in their very recent review [6]. Therefore, it is very important to prepare a "turn-on" sensory system with a lower initial fluorescence. The "dark background" fluorescence was achieved in our hybrid sensory system by preloading Cu^{2+} onto the amino receptor of tmeda-PPETE. The high sensitivity and selectivity toward Fe^{2+} of this fluorescence "turn-on" sensory system, as well as the possible mechanism, will be discussed.

3.1. Preparation of (x%-tmeda)-PPETEs

The preparation of the 2,5-dibrominated thiophene monomers with the *N*,*N*,*N*′-trimethylethylenediamino receptor connected to

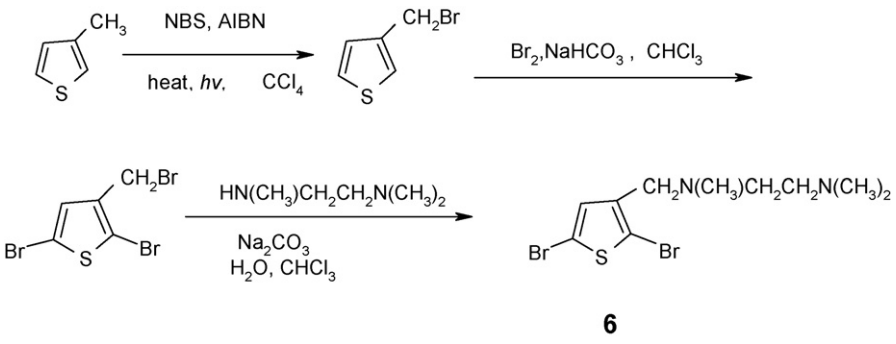

6

Scheme 3. Synthesis of amino receptor loaded monomer of tmeda-PPETE (see Ref. [79]).

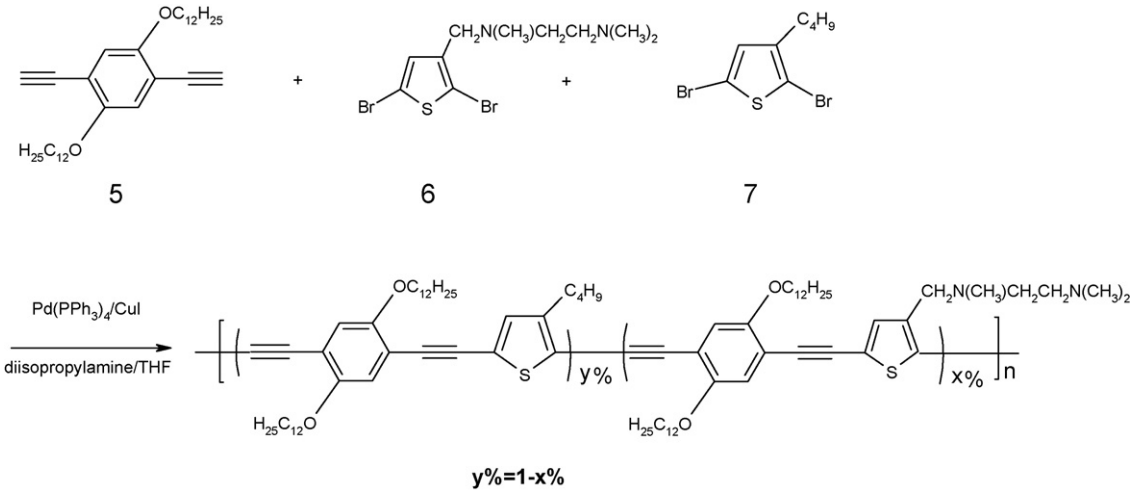

Scheme 4. The synthetic route of (x%-tmeda)-PPETEs with different receptor loading (see Ref. [79]). Mole ratio: (1) monomer **5**:monomer **6**:monomer **7** = 1:1:0 for (100%-tmeda)-PPETE (abbreviated as tmeda-PPETE in the following paragraphs); (2) monomer **5**:monomer **6**:monomer **7** = 1:0.50:0.50 for (50%-tmeda)-PPETE; (3) monomer **5**:monomer **6**:monomer **7** = 1:0.25:0.75 for (25%-tmeda)-PPETE; (4) monomer **5**:monomer **6**:monomer **7** = 1:0.125:0.875 for (12.5%-tmeda)-PPETE; (5) monomer **5**:monomer **6**:monomer **7** = 1:0:1 for model PPETE.

the thiophene ring by a methylene spacer loaded thiophene monomer **6** was synthesized as illustrated in Scheme 3. The 3-bromomethylthiophene was synthesized from commercially available 3-methylthiophene *via* a free radical reaction under nitrogen [86]. Bromination of this compound with Br_2 in the presence of $NaHCO_3$ gave 2,5-dibromo-3-bromomethyl-thiophene, which reacted with a secondary amine to give the desired monomer **6**.

The polymer series was synthesized by Pd-catalyzed polymerization and proceeded similar to the ttp-PPETE system described previously [57–60]. The various loading of the receptors was achieved by using different feed ratios of the monomers: 1,4-diethynyl-2,5-didodecyloxybenzene (monomer **5**), *N*-(2,5-dibromo-thiophen-3-ylmethyl)-*N*,*N*,*N*′-trimethylethane-1,2-diamine (monomer **6**), and 2,5-dibromo-3-butylthiophene (monomer **7**) (Scheme 4). Monomer **7** is commercially available. It is important to note that we assume the units with and without receptor to be randomly distributed due to the nature of the polymerization method employed. The model polymer we used here was slightly different from ttp-PPETE series, since here we use a butyl group on the thiophene ring instead of a dodecyl side chain. This was done based on the consideration that the butyl group was much closer to the *N*,*N*,*N*′-trimethylethane-1,2-diamino group in length.

Table 2
Quantum yields of fluorescence for (x%-tmeda)-PPETEs in THF solution at room temperature

Percentage of receptor loading (%)	Quantum yield
100	0.09
50	0.13
25	0.17
12.5	0.19
0	0.26

3.2. Photophysical properties of (x%-tmeda)-PPETEs

The absorption and emission spectra of the (x%-tmeda)-PPETEs are very similar to the model PPETE within experimental error (Fig. 15). As pointed out in the previous ttp-PPETE section, the absorption at ~450 nm in these polymers can be assigned to the π–π^* transition in the polymer backbone and both the emission maximum at 490 nm and the shoulder at 530 nm can be attributed to a single electronic transition with vibronic structure. Given the similarity in the photophysical properties, we conclude that these variations in receptor loading do not significantly influence the electronic structure of the lowest energy electronic transitions.

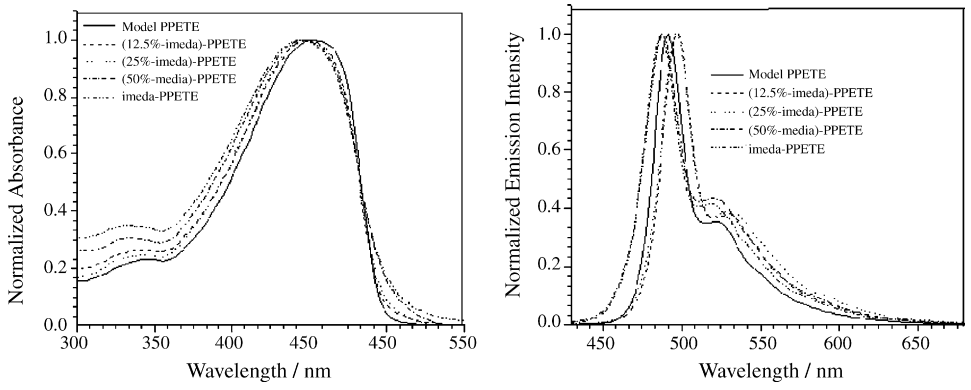

Fig. 15. Absorption (left) and emission spectra (right) of (x%-tmeda)-PPETEs in THF at 298 K (adapted from Ref. [85]).

The fluorescence quantum yields of the polymers (Table 2) decreased with increasing loading of the amino receptors compared to the model polymer. This was consistent with the expected quenching of the π–π^* excited state by the receptor. It is interesting to note that even for the 100% receptor loaded tmeda-PPETE, the fluorescence was not completely quenched. Several reasons could be used to describe this residual fluorescence. The first involves a kinetic competition between regular fluorescence and the intramolecular PET process [15,87]. When the PET quenching rate is slow, significant fluorescence can be observed. The second possibility involves the presence of localized fluorescence domains that are not coupled to a receptor. This has been described previously for conjugated polymers and results from structural inconsistencies in a random, non-rigid rod polymer where the amino receptors might be electronically insulated from the conjugated polymer backbone [15,49].

Since the receptor is expected to be randomly distributed along the polymer chain, localized fluorescence domains should increase with decreasing percent loading of the amino group. This is the most likely reason for the increase of fluorescence with decreasing amino group loading and consistent with this hypothesis. The emission decay in the emission lifetime measurement best fits a biexponential function for all polymers with 0.5 ns and 0.2 ns components. The lifetimes and the ratio between the two components showed no significant differences among these polymers. The invariant lifetimes are also consistent with the residual fluorescence resulting from localized fluorescence domains.

3.3. *Fluorescence enhancements of (x%-tmeda)-PPETEs upon cations*

Fig. 16(a) shows the trend of the intensity change when titrating different cations into tmeda-PPETE THF solution. Ca^{2+}, H^+ or Zn^{2+} showed much more sensitive fluorescence "turn-on" response than "Hg^{2+}" at the very lower cation concentration, though these cations did not yield maximum fluorescence enhancement as large as Hg^{2+} (Fig. 16b). For Ca^{2+}, H^+ or Zn^{2+}, the fluorescence enhancement saturation was reached at a very early stage (~5 μM), when the cation concentration was close to the concentration of the receptor unit in the solution. The polymer response toward different cations is expected, given the different association constants between cations and the amino receptor. We should emphasize here that the sensitivity of this kind of "turn-on" sensors is also be lower than the sensitivity of similar "turn-off" sensors, since the removal of a quencher site will need all the receptors to be fully loaded in the same quenching domain. This issue was discussed in detail by Swager and co-workers in their chemistry review paper published in 2007 [6]. Upon binding these cations, there is negligible shift in both the UV–vis absorption spectra and the excitation spectra, and also no change in lifetime. Emission profile shift is within experimental noise. On the basis of these photophysical studies, we can conclude that the ion complexation does not alter the conformation of the polymers in either ground state or excited state. Given the favorable driving force for electron transfer, these results are consistent with the intensity enhancement resulting from a "switching-off" of the PET process. Chelation-enhanced fluorescence (CHEF) also referred to this kind of fluorescence "turn-on" in small molecule systems [43,76–78].

Table 3
Maximum fluorescence enhancements for (x%-tmeda)-PPETEs upon titration of different cations

	Hg^{2+}	H^+	Zn^{2+}
(100%-tmeda)-PPETE (tmeda-PPETE)	2.65	1.87	1.68
(50%-tmeda)-PPETE	2.36	2.29	2.00
(25%-tmeda)-PPETE	2.02	2.02	1.60
(12.5%-tmeda)-PPETE	2.23	2.21	2.04

To investigate the sensitivity of these new chemosensory polymers with variable receptor loading, the influence of various cations (Hg^{2+}, Zn^{2+}) and protons on the fluorescence behavior of (x%-tmeda)-PPETEs was studied. All the polymers, except the model PPETE, had similar responses toward each cation and the results are summarized in Table 3. The maximum fluorescence enhancements for (x%-tmeda)-PPETEs at different receptor loadings show no large variations upon binding the same cation, considering the random distribution of receptor along the polymer backbone. Thus, in this fluorescence "turn-on" system, diluting the receptor along the polymer chain did not change the intensity enhancement of fluorescence. The concentration of each cation reaching maximum fluorescence enhancement or saturation is almost the same for different polymers. Therefore, the sensitivity did not increase with reducing the receptor loading as expected in an ideal conjugated polymer with PET system as a fluorescence "turn-on" system. In an ideal PET conjugated polymer–receptor system, PET quenching is very efficient and the energy migration is very rapid within the lifetime. An increased sensitivity would be expected upon reducing the receptor loading since fewer cations would be needed to completely turn on the fluorescence. In addition, the observation that the enhancement factor upon cation complexation for the 12.5%

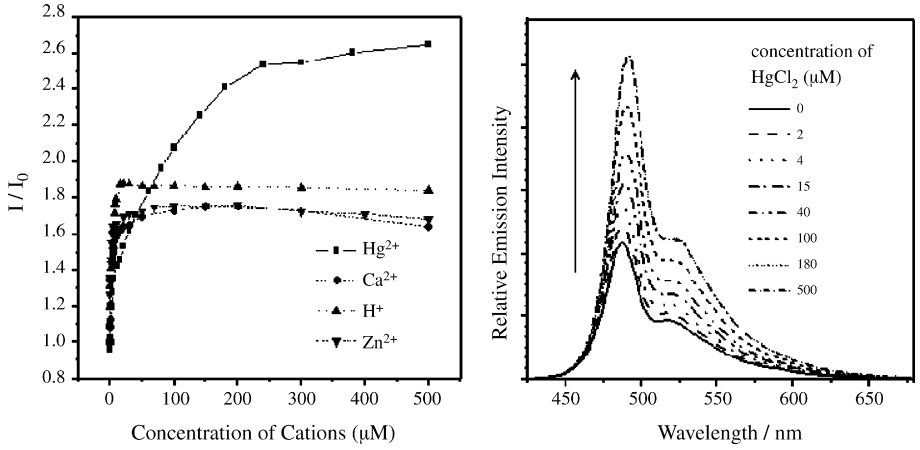

Fig. 16. (a) Fluorescence enhancement of tmeda-PPETE in THF upon addition of metal cations (left) and (b) emission spectra of tmeda-PPETE upon addition of different concentration of Hg^{2+}(right). Polymer concentration was held at 5 μM in receptor unit (adapted from Ref. [79]).

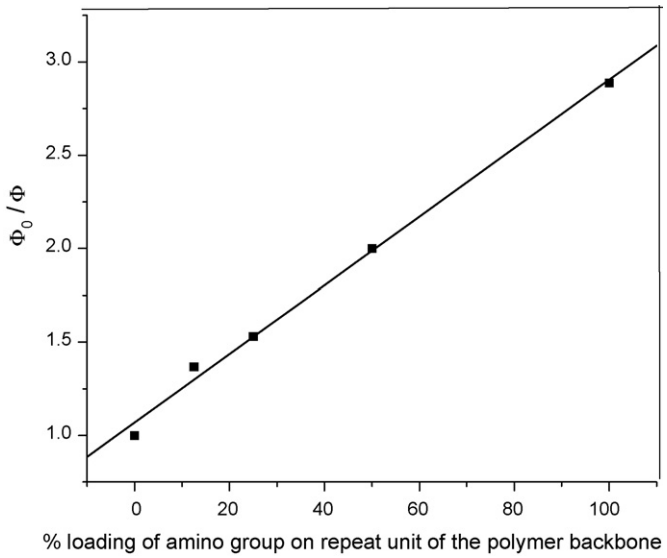

Fig. 17. Quantum yield ratios between the model PPETE and (x%-tmeda)-PPETEs vs. percent loading of amino group (adapted from Ref. [85])

loading of receptor units on the sample make the fluorescence of the polymer–cation complex somewhat greater than that of the model polymer. This was an unexpected result, but very reproducible. It is likely related to the different structures between the two polymers as synthesized and is currently under investigation.

3.4. Photoinduced electron transfer and energy migration analysis

In order to further understand the PET quenching of the polymer fluorescence by the amino group, an alternative analysis was undertaken using the Stern–Volmer quenching formalism [13,14]. Fig. 17 shows the Stern–Volmer fluorescence quantum yield ratios for the model PPETE as a function of the percent loading of the amino group. All the data fits a linear relationship, similar to Stern–Volmer quenching in a bimolecular fluorophore–quencher system.

Considering the quenching dynamics discussed in Section 2.3.1, a static quenching mechanism was expected given that the amino groups are covalently bound to PPETE fluorophore before excitation. The observed lack of change in the emission lifetime with change in the amino group loading in (x%-tmeda)-PPETEs is also consistent with the static quenching mechanism.

Based on the similarity of the absorption, emission spectra and emission lifetimes of this (x%-tmeda)-PPETE series, we conclude that all polymers have a similar delocalized exciton length. There is also no significant difference in the photoinduced electron transfer driving force for quenching within the series since the quencher is the same in all cases. This result is consistent with the earlier conclusion that the observed increase in fluorescence quantum yield with reduced receptor loading is due to residual fluorescence from localized domains on the polymer.

Excitation energy migration along the polymer backbone can lead to additional quenching of the polymer beyond the static process. In this (x%-tmeda)-PPETE system, the total quenching efficiency is not only decided by the PET quenching rate (k_{PET}) but also may affected by the rate of energy migration (k_{EM}).

As Webber and co-workers pointed out [69], in the case of a quencher residing permanently on a fluorescent polymer, if the energy migration is much slower than the quenching rate, $k_{EM} \ll k_{PET}$, any exciton that is locally excited at the quencher site or reaches the quencher site by energy migration is immediately quenched. Hence the energy migration on the polymer backbone improves total quenching efficiency.

If the energy migration is faster than the quenching rate, $k_{EM} \geq k_{PET}$, the energy migration may remove the exciton from the quencher site before quenching takes place. The energy migration enhanced quenching might not be observed. This situation is very similar to a dynamic quenching process induced by the diffusion in small bimolecular systems. The only difference is that in our case the exciton "diffuses" through energy migration instead of the quencher diffusing to the fluorophore. This situation can not be true in the (x%-tmeda)-PPETE system because it is known that the dynamic quenching would lead to a decreased lifetime with increasing quencher loading. Since the lifetimes are invariant, we can conclude that $k_{EM} \ll k_{PET}$ in this system.

From the linear Stern–Volmer quenching in Fig. 17 and the fact that the polymer fluorescence lifetime has no amino loading dependence, we can deduce that the energy migration cannot be very fast within emissive lifetime. Otherwise, a small amount of the amino group would quench the polymer fluorescence completely. However, energy migration enhanced fluorescence quenching was still observed in (x%-tmeda)-PPETE, since the fluorescence of the 12.5% amino receptor loaded polymer was quenched by 27% according quantum yields. If we correct for the residual fluorescence, the 12.5% amino receptor actually quenched about 41% of the quenchable fluorescence on the polymer backbone. From this set of observations we conclude that $k_{EM} \leq 1/\tau_0$ ($\sim 10^9\ s^{-1}$) $\ll k_{PET}$. Cation titrations (see Section 3.3) of this series of polymers showed no sensitivity enhancements upon reduced receptor loading which is consistent with the relatively sluggish energy migration along the polymer backbone. We may conclude that higher sensitivity might be achieved in systems with better energy migration along the polymer backbone.

3.5. Inorganic/organic hybrid polymer chemosensors

The tmeda-PPETE showed varying fluorescence "turn-on" behavior in the presence of cations including protons, Zn^{2+}, Ca^{2+}, and Hg^{2+}, as described previously. However, the overall sensitivity was limited by the relatively high background fluorescence with a quantum yield of 0.09 [79].

With the goal of achieving a more selective and sensitive fluorescence "turn-on" sensory system, a more systematic investigation was carried out for this tmeda-PPETE system [88]. The polymer in THF was titrated with a series of cations: including Cu^{2+}, Li^+, Na^+, K^+, Mg^{2+}, Mn^{2+}, Fe^{2+}, Co^{2+}, $Ni^{2+}$and Cd^{2+}, in addition to the Zn^{2+}, Hg^{2+}, Ca^{2+} and H^+. Most cations turned on the fluorescence of tmeda-PPETE to varying degrees. Interestingly, Cu^{2+} was found to exhibit a noteworthy exception to the fluorescence behavior in this system [88].

Based on the Cu^{2+} quenching, we hypothesized that an inorganic/organic hybrid system may provide for enhanced sensitivity by preloading Cu^{2+} onto the amino receptor to totally quench the initial background fluorescence. Thus a fluorescence "turn-on" chemosensory system for cations based on a tmeda-PPETE/Cu^{2+} hybrid system was designed [88].

The tmeda-PPETE/Cu^{2+} hybrid system was prepared from THF solutions of tmeda-PPETE with a repeat unit concentration of 5 μM. $CuCl_2$ was added from aqueous stock solution to reach a final concentration of 5 μM and to achieve a 1:1 ratio of Cu^{2+} to receptor.

The titration of Fe^{2+} was carried out by adding small aliquots of $FeCl_2$ aqueous stock solution into the THF solutions containing the tmeda-PPETE/Cu^{2+} hybrid system. We observed a greater than 100-fold enhancement in the fluorescence intensity upon titration of 10 μM aqueous ferrous chloride (Fig. 18). During the titration, the emission maximum did not shift and the UV–vis spectra showed

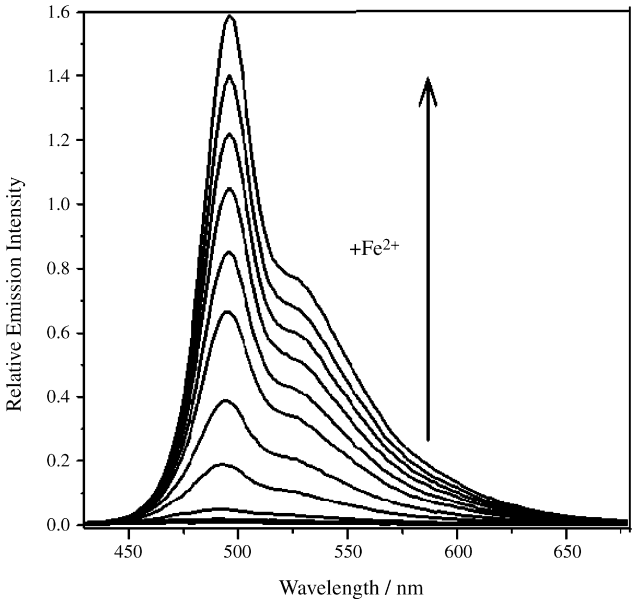

Fig. 18. Fluorescence response following excitation at 408 nm from tmeda-PPETE/Cu^{2+} solutions upon addition of Fe^{2+} aqueous solution. The concentrations of the Fe^{2+} for the spectra (from bottom to top) were 0, 1, 2, 3, 4, 5, 6, 7, 8 and 10 μM. The concentrations of tmeda-PPETE (with respect to the repeat unit) and Cu^{2+} were fixed at 5 μM (adapted from Ref. [88]).

negligible changes. This suggests no significant change in the overall electronic structure of the polymer upon addition of Fe^{2+}. The final fluorescence intensity of the titrated solution was almost the same as for the titration of the pure polymer in the absence of Cu^{2+}. Based on these results we assume that the Fe^{2+} has displaced the Cu^{2+} from the receptor. Attempts to directly observe the binding event by NMR and EPR have to date proved unsuccessful.

For comparison purposes, the influence of some other cations, such as Ca^{2+} Hg^{2+}, Zn^{2+}, Ni^{2+}, Mn^{2+} and H^+ were also investigated and the data was collected based on the relative change in fluorescence intensity, I/I_0. In each case, a total amount of 10 μM of cations was added into the tmeda-PPETE/Cu^{2+} solution.

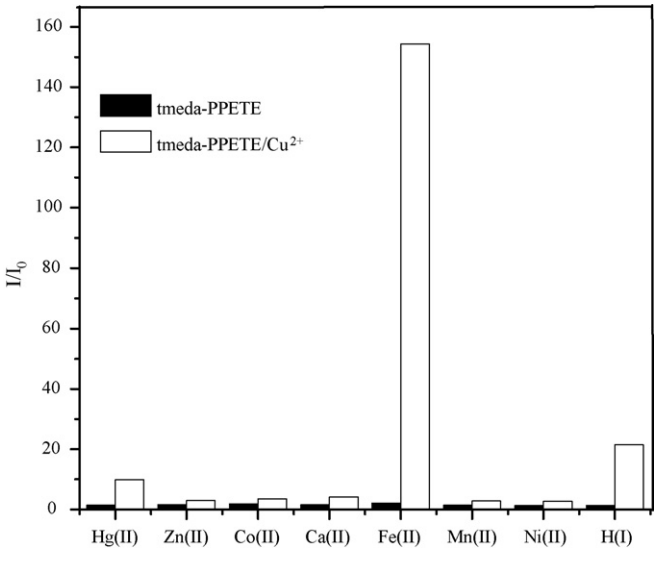

Fig. 19. Fluorescence response of tmeda-PPETE/Cu^{2+} (white) or tmeda-PPETE (black) to various 10 μM cations in room temperature solution. The concentrations of tmeda-PPETE (with respect to the repeat unit) and Cu^{2+} were fixed at 5 μM (adapted from Ref. [88]).

As shown in Fig. 19, the system is highly selective for Fe^{2+} with fluorescence enhancements of 150-fold. No other metal cations showed such a significant response. The one analyte sample that did respond similarly was Hg^{2+} with only a 10-fold enhancement. The addition of all the cations into pure tmeda-PPETE THF solution is also shown for comparison. Results showed there was no significant difference in fluorescence enhancement among any of these cations for the pure chemosensor polymer. In all cases, the fluorescence enhancement was significantly smaller for the model compared to the tmeda-PPETE/Cu^{2+} system. From these results, it was concluded that the high sensitivity and selectivity required the polymer/Cu^{2+} hybrid. It was also demonstrated that the observed enhancement was not the result of simple cation hydrolysis mechanisms [89], based on the fact that similar titration of H^+ solution only resulted in about 20-fold of fluorescence enhancement.

The tmeda-PPETE/Cu^{2+} system was highly selective toward Fe^{2+} cations in solution. Since this selectivity is not present for the parent tmeda-PPETE solutions, it must not be based simply on the association constant between the receptor ligand and the cation. This would typically be expected for a simple host–guest interaction, in this case between the Lewis acid metal ion and the Lewis base receptor. It is likely that the selectivity is related to the relative ability of the cations to replace the Cu^{2+} already in coordination with the receptor. Competitive binding has previously been observed in small molecule sensors and other host–guest interactions [90,91]. The relative coordination of metal cations can often be related to their Lewis acid–base properties. However, Fe^{2+} and other cations do not follow a consistent trend so more work is necessary to specifically identify the mode of action for the selectivity.

4. Conclusion

Several new sensory systems for the transition metal cations detection were created in our group, based on the successful combination of coordination chemistry between the receptor and transition metal with molecular wire concept for conjugated polymer. The additional discussion about the system helped us further understand the factors, such as the energy migration along the polymer backbone, the interaction between the receptor and analytes and the quenching mechanism, which influence the sensing performance and may be useful for further design new classes of chemosensors.

Acknowledgements

This research was supported in part by a grant from the National Institute of Health (NIH grant 1R15ES10106-01) and the Research Foundation of the State University of New York. The authors also thank S. Pinnock for useful discussions.

References

[1] B.R. Eggins, Chemical Sensors and Biosensors, John Wiley, New York, 2002.
[2] G. Harsányi, Sensors in Biomedical Applications: Fundamentals, Technology & Applications, Technomic Pub. Co., Lancaster, PA, 2000.
[3] O.S. Wolfbeis, Anal. Chem. 78 (12) (2006) 3859.
[4] A.T. Wright, E.V. Anslyn, Chem. Soc. Rev. 35 (1) (2006) 14.
[5] Z. Juan, T.M. Swager, Adv. Polym. Sci. 177 (2005) 151.
[6] S.W. Thomas, G.D. Joly, T.M. Swager, Chem. Rev. 107 (4) (2007) 1339.
[7] A.W. Czarnik, Fluorescent Chemosensors for Ion and Molecule Recognition, American Chemical Society, Washington, DC, 1993.
[8] A.P. de Silva, H.Q.N. Gunaratne, T. Gunnlaugsson, A.J.M. Huxley, C.P. McCoy, J.T. Rademacher, T.E. Rice, Chem. Rev. 97 (5) (1997) 1515.
[9] R. Martinez-Manez, F. Sancenon, Chem. Rev. 103 (11) (2003) 4419.
[10] B. Valeur, I. Leray, Coord. Chem. Rev. 205 (1) (2000) 3.
[11] T. Gunnlaugsson, M. Glynn, G.M. Tocci, P.E. Kruger, F.M. Pfeffer, Coord. Chem. Rev. 250 (23/24) (2006) 3094.
[12] P. Jiang, Z. Guo, Coord. Chem. Rev. 248 (1/2) (2004) 205.

[13] J.R. Lakowicz, Principles of Fluorescence Spectroscopy, Kluwer Academic/Plenum, New York, 1999.
[14] N.J. Turro, Modern Molecular Photochemistry, University Science Books Sauslito, California, 1991.
[15] J. Guillet, Polymer Photophysics and Photochemistry, Cambridge University Press, Cambridge, UK, 1985.
[16] C.K. Chiang, C.R. Fincher, Y.W. Park, A.J. Heeger, H. Shirakawa, E.J. Louis, S.C. Gau, A.G. MacDiarmid, Phys. Rev. Lett. 39 (17) (1977) 1098.
[17] C.K. Chiang, M.A. Druy, S.C. Gau, A.J. Heeger, E.J. Louis, A.G. MacDiarmid, Y.W. Park, H. Shirakawa, J. Am. Chem. Soc. 100 (3) (1978) 1013.
[18] J.H. Burroughes, D.D.C. Bradley, A.R. Brown, R.N. Marks, K. Mackay, R.H. Friend, P.L. Burns, A.B. Holmes, Nature 347 (6293) (1990) 539.
[19] P.L. Burn, A. Kraft, D. Baigent, D.D.C. Bradley, A.R. Brown, R.H. Friend, R.W. Gymer, A.B. Holmes, R.W. Jackson, J. Am. Chem. Soc. 115 (22) (1993) 10117.
[20] A. Kraft, A.C. Grimsdale, A.B. Holmes, Angew. Chem. Int. Ed. 37 (4) (1998) 402.
[21] R.H. Friend, R.W. Gymer, A.B. Holmes, J.H. Burroughes, R.N. Marks, C. Taliani, D.D.C. Bradley, D.A. Dos Santos, J.L. Bredas, M. Logdlund, W.R. Salaneck, Nature 397 (6715) (1999) 121.
[22] J.H. Alan, Angew. Chem. Int. Ed. 40 (14) (2001) 2591.
[23] A.C. Arango, L.R. Johnson, V.N. Bliznyuk, Z. Schlesinger, S.A. Carter, H.H. Höhold, Adv. Mater. 12 (22) (2000) 1689.
[24] S.A. McDonald, G. Konstantatos, S.G. Zhang, P.W. Cyr, E.J.D. Klem, L. Levina, E.H. Sargent, Nat. Mater. 4 (2) (2005), 138-U14.
[25] K.M. Coakley, M.D. McGehee, Chem. Mater. 16 (23) (2004) 4533.
[26] A.M. Ramos, M.T. Rispens, J.K.J. van Duren, J.C. Hummelen, R.A.J. Janssen, J. Am. Chem. Soc. 123 (27) (2001) 6714.
[27] E.W.H. Jager, O. Inganäs, I. Lundström, Adv. Mater. 13 (1) (2001) 76.
[28] P. Burgmayer, R.W. Murray, J. Am. Chem. Soc. 104 (22) (1982) 6139.
[29] R. Gangopadhyay, A. De, Chem. Mater. 12 (3) (2000) 608.
[30] W.H. Meyer, Adv. Mater. 10 (6) (1998) 439.
[31] C.D. Dimitrakopoulos, P.R.L. Malenfant, Adv. Mater. 14 (2) (2002) 99.
[32] T.M. Swager, Acc. Chem. Res. 31 (5) (1998) 201.
[33] D.T. McQuade, A.E. Pullen, T.M. Swager, Chem. Rev. 100 (7) (2000) 2537.
[34] B.S. Gaylord, M.R. Massie, S.C. Feinstein, G.C. Bazan, Proc. Natl. Acad. Sci. U.S.A. 102 (1) (2005) 34.
[35] S. Kumaraswamy, T. Bergstedt, X.B. Shi, F. Rininsland, S. Kushon, W.S. Xia, K. Ley, K. Achyuthan, D. McBranch, D. Whitten, Proc. Natl. Acad. Sci. U.S.A. 101 (20) (2004) 7511.
[36] A. Petrella, M. Tamborra, M.L. Curri, P. Cosma, M. Striccoli, P.D. Cozzoli, A. Agostiano, J. Phys. Chem. B 109 (4) (2005) 1554.
[37] S.J. Dwight, B.S. Gaylord, J.W. Hong, G.C. Bazan, J. Am. Chem. Soc. 126 (51) (2004) 16850.
[38] A. Watt, E. Thomsen, P. Meredith, H. Rubinsztein-Dunlop, Chem. Commun. 20 (2004) 2334.
[39] H.A. Ho, M. Leclerc, J. Am. Chem. Soc. 126 (5) (2004) 1384.
[40] H.-A. Ho, M. Boissinot, M.G. Bergeron, G. Corbeil, K. Dore, D. Boudreau, M. Leclerc, Angew. Chem. Int. Ed. 41 (9) (2002) 1548.
[41] J. Li, Y. Pang, Macromolecules 31 (17) (1998) 5740.
[42] Y. Pang, J. Li, B. Hu, F.E. Karasz, Macromolecules 31 (19) (1998) 6730.
[43] A.W. Czarnik, Acc. Chem. Res. 27 (10) (1994) 302.
[44] M.D. Disney, J. Zheng, T.M. Swager, P.H. Seeberger, J. Am. Chem. Soc. 126 (41) (2004) 13343.
[45] J.H. Wosnick, C.M. Mello, T.M. Swager, J. Am. Chem. Soc. 127 (10) (2005) 3400.
[46] J.S. Yang, T.M. Swager, J. Am. Chem. Soc. 120 (46) (1998) 11864.
[47] Q. Zhou, T.M. Swager, J. Am. Chem. Soc. 117 (50) (1995) 12593.
[48] Q. Zhou, T.M. Swager, J. Am. Chem. Soc. 117 (26) (1995) 7017.
[49] T.A. Skoheim, R.L. Elsenbaumer, J.R. Reynolds, Handbook of Conducting Polymers, second ed., Marcel Dekker, New York, NY, 1998.
[50] M. Leclerc, Adv. Mater. 11 (18) (1999) 1491.
[51] I. Levesque, M. Leclerc, Chem. Mater. 8 (12) (1996) 2843.
[52] B. Wang, M.R. Wasielewski, J. Am. Chem. Soc. 119 (1) (1997) 12.
[53] L. Chen, D.W. McBranch, H.-L. Wang, R. Helgeson, F. Wudl, D.G. Whitten, Proc. Natl. Acad. Sci. U.S.A. 96 (22) (1999) 12287.
[54] US EPA, Federal Register 44:69464 ed., EPA, 1979.
[55] J.-P. Sauvage, W. Hosseini, Comprehensive Coordination Chemistry, vol. 9, Pergamon, Oxford, 1996.
[56] M. Kimura, T. Horai, K. Hanabusa, H. Shirai, Adv. Mater. 10 (6) (1998) 459.
[57] Y. Zhang, C.B. Murphy, W.E. Jones, Macromolecules 35 (3) (2002) 630.
[58] C.B. Murphy, Y. Zhang, T. Troxler, V. Ferry, J.J. Martin, W.E. Jones, J. Phys. Chem. B 108 (5) (2004) 1537.
[59] S.E. Angell, Ruthenium(II) Bipyridyl Complexes Containing Hemilabile Ligand and Fluorescent Conjugated Polymers as Small Molecule Sensors, M.S. Thesis, State University of New York at Binghamton, Binghamton, NY, 2005.
[60] M.F.L. Parker, Rational Design and Synthesis of Fluorescent Conjugated Polymers for Probing Energy Transfer Mechanism, M.S. Thesis, State University of New York at Binghamton, Binghamton, NY, 2005.
[61] E. Negishi, Handbook of Organopalladium Chemistry for Organic Synthesis, Wiley–Interscience, New York, 2002.
[62] J. Tsuji, Palladium Reagents and Catalysts: New Perspectives for the 21st Century, 2nd ed., John Wiley and Sons, Chichester; Hoboken, NJ, 2004.
[63] T. Yamamoto, K. Honda, N. Ooba, S. Tomaru, Macromolecules 31 (1) (1998) 7.
[64] T.M. Swager, C.J. Gil, M.S. Wrighton, J. Phys. Chem. 99 (14) (1995) 4886.
[65] J. Boutagy, R. Thomas, Chem. Rev. 74 (1) (1974) 87.
[66] J.P. Collin, S. Guillerez, J.P. Sauvage, F. Barigelletti, L. Decola, L. Flamigni, V. Balzani, Inorg. Chem. 30 (22) (1991) 4230.
[67] L. Chen, S. Xu, D. McBranch, D. Whitten, J. Am. Chem. Soc. 122 (38) (2000) 9302.
[68] R.M. Jones, T.S. Bergstedt, D.W. McBranch, D.G. Whitten, J. Am. Chem. Soc. 123 (27) (2001) 6726.
[69] Y. Itoh, K. Kamioka, S.E. Webber, Macromolecules 22 (6) (1989) 2851.
[70] H. Tong, Y.N. Hong, Y.Q. Dong, M. Haussler, J.W.Y. Lam, Z. Li, Z.F. Guo, Z.H. Guo, B.Z. Tang, Chem. Commun. 35 (2006) 3705.
[71] H. Tong, L. Wang, X. Jing, F. Wang, Macromolecules 36 (8) (2003) 2584.
[72] T.L. Andrew, T.M. Swager, J. Am. Chem. Soc. 129 (23) (2007) 7254.
[73] D.T. McQuade, A.H. Hegedus, T.M. Swager, J. Am. Chem. Soc. 122 (49) (2000) 12389.
[74] K. Rurack, M. Kollmannsberger, U. Resch-Genger, J. Daub, J. Am. Chem. Soc. 122 (5) (2000) 968.
[75] E.U. Akkaya, M.E. Huston, A.W. Czarnik, J. Am. Chem. Soc. 112 (9) (1990) 3590.
[76] M.E. Huston, E.U. Akkaya, A.W. Czarnik, J. Am. Chem. Soc. 111 (23) (1989) 8735.
[77] M.E. Huston, K.W. Haider, A.W. Czarnik, J. Am. Chem. Soc. 110 (13) (1988) 4460.
[78] S.A. Van Arman, A.W. Czarnik, J. Am. Chem. Soc. 112 (13) (1990) 5376.
[79] L.J. Fan, Y. Zhang, W.E. Jones, Macromolecules 38 (7) (2005) 2844.
[80] A.P. de Silva, H.Q.N. Gunaratne, P.L.M. Lynch, A.J. Patty, G.L. Spence, J. Chem. Soc., Perkin Trans. (9) (1993) 1611.
[81] G. Jones, S.F. Griffin, C.Y. Choi, W.R. Bergmark, J. Org. Chem. 49 (15) (1984) 2705.
[82] D. Rehm, A. Weller, Isr. J. Chem. 8 (1970) 259.
[83] A. Weller, Pure Appl. Chem. (16) (1968) 115.
[84] D.C. Harris, Quantitative Chemical Analysis, 5th ed., W.H. Freeman and Company, New York, 1999.
[85] L.J. Fan, W.E. Jones, J. Phys. Chem. B 110 (15) (2006) 7777.
[86] S.S. Mandal, J. Chakraborty, A. De, J. Chem. Soc., Perkin Trans. 1 (18) (1999) 2639.
[87] P. Ghosh, P.K. Bharadwaj, J. Roy, S. Ghosh, J. Am. Chem. Soc. 119 (49) (1997) 11903.
[88] L.J. Fan, W.E. Jones, J. Am. Chem. Soc. 128 (21) (2006) 6784.
[89] C.F. Banes, R.E. Mesmer, The Hydrolysis of Cations, Wiley–Interscience, New York, 1976.
[90] S. Wiskur, H. Ait-Haddou, E. Anslyn, J. Lavigne, Acc. Chem. Res. 34 (12) (2001) 963.
[91] B.T. Nguyen, E.V. Anslyn, Coord. Chem. Rev. 250 (23/24) (2006) 3118.